SCIENCE CHINA
Physics, Mechanics & Astronomy

• Article •
Special Issue: Physical Mechanics

June 2012 Vol.55 No.6: 918–926
doi: 10.1007/s11433-012-4744-3

Thermodynamic properties and constitutive relations of crystals at finite temperature

TANG QiHeng, WANG TzuChiang*, SHANG BaoShuang & LIU Feng

State Key Laboratory of Nonlinear Mechanics, Institute of Mechanics, Chinese Academy of Sciences, Beijing 100190, China

Received December 1, 2011; accepted February 17, 2012; published online April 18, 2012

The dynamics equation for each individual atom is established directly around the equilibrium state of the system of N atoms based on the inter-atomic potential energy of EAM model. Using the theory of lattice dynamics and periodical boundary condition, the $3N\times3N$ stiffness matrix in eigen equations of vibration frequencies for a parallelepiped crystal is reduced to a $3n\times3n$ matrix of eigen equations of vibration frequencies for a unit lattice. The constitutive relation of the crystal at finite temperature is extracted based on the quantum-mechanical principle. The thermodynamic properties and the stress-strain relationships of crystal Cu with large plastic deformation at different temperatures are calculated, the calculation results agree well with experimental data.

lattice wave theory, molecular dynamics, thermodynamic properties, constitutive model, interatomic potential

PACS number(s): 81.05.Bx, 65.40.-b, 63.90.+t

Citation: Tang Q H, Wang T C, Shang B S, et al. Thermodynamic properties and constitutive relations of crystals at finite temperature. Sci China-Phys Mech Astron, 2012, 55: 918–926, doi: 10.1007/s11433-012-4744-3

Rapid developments of nano-and micro technology such as computer chips, powerful microscopy tools, nano- and micro- electromechanical systems (NEMS and MEMS) have shifted the research of materials sciences, physics and mechanics to the nano- and micro- scale. Classical continuum methods encounter great challenge, since they cannot capture the essential features of many effects in the nanoscale [1]. In this case, several modeling methods including *ab initial* calculation, molecular dynamics (MD) and Monte Carlo (MC) simulations are quickly developed. But the computation cost is quite large for several hundred electrons (in *ab initial* calculations) and several million atoms (in MD and MC simulations). Hence one scale methods are impractical for engineering application.

Many multi-scale modeling methods to link atomic physics with continuum theories have been proposed. The quasi-continuum method was originally proposed by Tadmor, Ortiz and Phillips in 1996 [2,3]. The QC method employs the continuum framework to reduce the degrees of freedom without losing the atomistic features in the critical regions. QC method is developed and used to study many interesting problems, including defects in materials [2], interfacial deformation [4], fracture and plasticity [5,6], multiscale plasticity behavior [7] and carbon nano-tube mechanical properties [8]. Gao and Klein [9] and Klein and Gao [10] proposed a virtual-internal-bond model which incorporates the atomistic interaction into continuum simulation to study the crack nucleation and growth. But the original QC method is limited to zero temperature, and now it has been developed to take into account the effect of finite temperature [11–13] within the framework of local quasi-harmonic approximation. Dupuy et al. [14] developed a coarse-grained alternative for molecular dynamics of solids.

The local quasi-harmonic method (LQHM) is simple and efficient, but the results given by LQHM can be inaccurate

*Corresponding author (email: tcwang@imech.ac.cn)

due to its neglecting completely the interaction of different atoms.

The harmonic model (HM) has been proposed by Born and Huang [15]. The HM model directly computes all the vibration frequencies of the crystal. But the vibration frequencies are the eigenvalues of a $3N\times3N$ force constant matrix.

According to the harmonic model, the total potential energy and the vibration frequencies are evaluated at the equilibrium position of the system. In a quasi-harmonic model (QHM), the quasi equilibrium position of the system is characterized by the lattice constant, which is a function of temperature. Therefore the total potential energy and the vibration frequencies are also functions of temperature [16,17].

Tang et al. [17] proposed a quasi-harmonic method in the reciprocal space (k-space), namely the QHMK model, to calculate the Helmholtz free energy based on the quantum-mechanical principle of lattice dynamics and the inter-atomic potential. Zhao et al. [18] employed the QMMK model to investigate the thermo properties of silicon under different strains. QHMK model is accurate and efficient.

In this paper, first, the exact dynamics equation for each individual atom is established directly around the equilibrium state of the system of N atoms in terms of the inter-atomic forces which can be expressed as the first derivative of inter-atomic potential. Second, by using the theory of lattice dynamics [15] and periodical boundary condition, the $3N\times3N$ stiffness matrix in the frequency equations of the parallelepiped crystal is reduced to a $3n\times3n$ stiffness matrix in the frequency equations of a unit cell, with n being the number of atoms in the unit cell.

Along this line, the $3N$ frequencies of the parallelepiped crystal are completely obtained. The constitutive relation of crystal at finite temperature is extracted based on the quantum-mechanical principle. Finally the present method is extended to include the effect of plastic deformation.

The paper is divided into 5 sections. Sect. 2 introduces the basic principles of the present method. Thermodynamic properties of crystal of Cu are given in sect. 3. The thermal stress of crystal Copper is given in sect. 4. Sect. 5 presents the conclusion and discussion.

1 Basic principles

A parallelepiped crystal (rectangular or inclined) which is made up by repetitions of the Bravais's lattice is taken to be a representative volume element. The parallelepiped crystal is subjected to a homogeneous deformation.

1.1 Lattice dynamics

Let us consider a system of N-atoms of perfect crystal. The total energy function of the system can be expressed as the sum of each atom individually,

$$U_{\text{tot}} = \sum_{i=1}^{N} U_i, \tag{1}$$

where U_i is the potential energy of atom i.

Within the atomistic model of Embedded Atom Method (EAM), the potential energy U_i is given by Daw and Baskes [19]:

$$U_i = \frac{1}{2}\sum_{j\neq i}\phi_{ij}(r_{ij}) + F_i(\bar{\rho}_i), \tag{2}$$

where $F_i(\bar{\rho}_i)$ is the embedded energy, which depends on the spherical averaged electric density $\bar{\rho}_i$, and it can be expressed as:

$$\bar{\rho}_i = \sum_{j\neq i}\rho_j(r_{ij}), \tag{3}$$

where $\rho_j(r_{ij})$ is the electric density distribution on the position of atom i from the neighbor atom j. Obviously the pair potential $\phi_{ij}(r_{ij})$ depends only on the bond length.

The force acting on atom i equals

$$\begin{aligned}\boldsymbol{f}_i &= -\frac{\partial U_{\text{tot}}}{\partial \boldsymbol{u}_i}\\ &= -\sum_{j\neq i}\{\phi'_{ij}(r_{ij}) + [F'_i(\bar{\rho}_i)\rho'_j(r_{ij}) + F'_j(\bar{\rho}_j)\rho'_i(r_{ji})\}\frac{\partial r_{ij}}{\partial \boldsymbol{u}_i}.\end{aligned}$$

The static equilibrium equation of atom k can be written as:

$$\sum_{j\in\Omega_k}\frac{f_{kj}\left(r_{kj}\right)}{r_{kj}}\boldsymbol{r}_{kj} = 0, \tag{4}$$

where $f\left(r_{kj}\right)$ is the interaction force between atom k and atom j, which takes the form:

$$f_{kj}(r_{kj}) = \phi'_{kj}(r_{kj}) + [F'_k(\bar{\rho}_k)\rho'_j(r_{kj}) + F'_j(\bar{\rho}_j)\rho'_k(r_{jk})]. \tag{5}$$

At finite temperature, atoms vibrate thermodynamically around their equilibrium positions with high frequencies and small amplitudes as shown in Figure 1.

The force acting on atom k becomes

$$\sum_{j\in\Omega_k}\frac{f_{kj}\left(r'_{kj}\right)}{r'_{kj}}\boldsymbol{r}'_{kj}.$$

The radius vector $\boldsymbol{r}'_{kj}$ from k to atom j takes the form:

$$\boldsymbol{r}'_{kj} = \boldsymbol{r}_{kj} + \boldsymbol{u}_j - \boldsymbol{u}_k.$$

The dynamics equation of atom k can be expressed as:

$$m_k\ddot{\boldsymbol{u}}_k(\boldsymbol{R}_n) = \sum_{j\in\Omega_k}\frac{f_{kj}\left(r_{kj}\sqrt{1+2\varepsilon_{kj}}\right)}{r_{kj}\sqrt{1+2\varepsilon_{kj}}}\left(\boldsymbol{r}_{kj} + \boldsymbol{u}_j - \boldsymbol{u}_k\right), \tag{6}$$

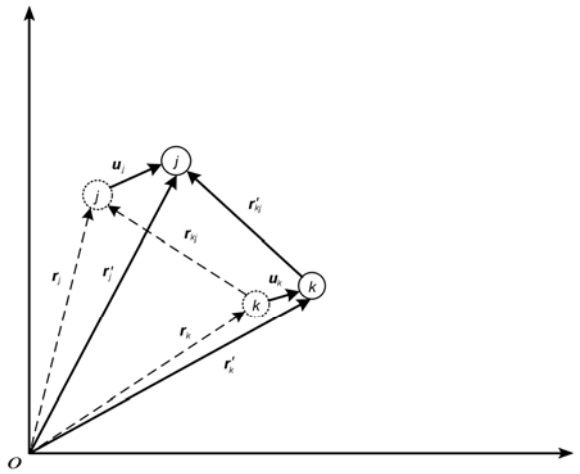

Figure 1 Schematic diagram of atom positions (solid circles) surrounding their equilibrium positions (dashed circles), $\boldsymbol{r}_{kj}$ is the radius vector from atom k to atom j in the equilibrium position, $\boldsymbol{u}_j$ and $\boldsymbol{u}_k$ are the displacements of atom j, k due to thermo vibration, and $\boldsymbol{r}'_{kj}$ is the radius vector from atom k to atom j out of equilibrium position.

where Ω_k represents a set of all atoms which have interaction with atom k, $k = 0, \overline{1}, \overline{2}, \cdots$ are the numbers of the atoms within the unit cell, j=1, 2, 3, $\cdots$ are the numbers of the atoms within the set Ω_k, and $\boldsymbol{R}_n$ is the position vector of the origin of the unit cell. The ε_{kj} equals

$$\varepsilon_{kj} = \frac{\left(\boldsymbol{u}_j - \boldsymbol{u}_k\right)\cdot \boldsymbol{e}_{kj}}{r_{kj}} + \frac{1}{2}\frac{\left(\boldsymbol{u}_j - \boldsymbol{u}_k\right)\cdot\left(\boldsymbol{u}_j - \boldsymbol{u}_k\right)}{r_{kj}^2}, \tag{7}$$

where $\boldsymbol{e}_{kj} = \boldsymbol{r}_{kj} / r_{kj}$ is the unit vector along the vector $\boldsymbol{r}_{kj}$ direction.

Eq. (6) is the exact dynamic equation of atom k without any approximation.

If the term $|(\boldsymbol{u}_j - \boldsymbol{u}_k)/r_{kj}|$ is small enough, then eq. (6) becomes

$$m_k \ddot{\boldsymbol{u}}_k(\boldsymbol{R}_n) = \sum_{j\in\Omega_k}\left\{\frac{f\left(r_{kj}\right)}{r_{kj}}\left(\boldsymbol{u}_j - \boldsymbol{u}_k\right) + \left(f'\left(r_{kj}\right) - \frac{f\left(r_{kj}\right)}{r_{kj}}\right)\boldsymbol{e}_{kj}\left[\left(\boldsymbol{u}_j - \boldsymbol{u}_k\right)\cdot\boldsymbol{e}_{kj}\right]\right\}. \tag{8}$$

Eq. (8) is the harmonic approximation of the dynamic equation (6) of atom k that has been proposed by Tang and Wang [20]. Eq. (8) can be rewritten as follows:

$$m_k\ddot{\boldsymbol{u}}_k = \sum_{j\in\Omega_k}\boldsymbol{K}_{kj}\cdot\left(\boldsymbol{u}_j - \boldsymbol{u}_k\right), \tag{9}$$

where

$$\boldsymbol{K}_{kj}(r_{kj}) = \frac{f_{kj}\left(r_{kj}\right)}{r_{kj}}\boldsymbol{I} + \left[f'_{kj}\left(r_{kj}\right) - \frac{f_{kj}\left(r_{kj}\right)}{r_{kj}}\right]\boldsymbol{e}_{kj}\otimes\boldsymbol{e}_{kj}, \tag{10}$$

where $\boldsymbol{I}$ is the second-order unit tensor.

The solution to dynamic equation (9) can be expressed as [21,22]:

$$\boldsymbol{u}_j = \boldsymbol{A}_j \mathrm{e}^{\mathrm{i}(\omega t - (\boldsymbol{R}_n + \boldsymbol{r}_{kj})\cdot\boldsymbol{q})}, \tag{11}$$

where $\boldsymbol{q}$ is the wave vector. Substituting eq. (11) into eq. (9), one obtains

$$-m_k\omega^2\boldsymbol{A}_k = \sum_{j=\Omega_k}\boldsymbol{K}_{kj}\cdot[\boldsymbol{A}_j\mathrm{e}^{-\mathrm{i}\boldsymbol{r}_{kj}\cdot\boldsymbol{q}} - \boldsymbol{A}_k]. \tag{12}$$

If per unit cell contains only one atom, eq. (12) becomes

$$-m\omega^2\boldsymbol{A} = \sum_{j=\Omega_k}\boldsymbol{K}_{kj}(\mathrm{e}^{-\mathrm{i}\boldsymbol{r}_{kj}\cdot\boldsymbol{q}} - 1)\cdot\boldsymbol{A}. \tag{13}$$

Eq. (13) is the eigen-equation of three-dimensional monatomic crystal.

1.2 The solution of molecular dynamics

The solution of dynamic equations of N atom system takes the form:

$$\boldsymbol{u}(\boldsymbol{R}) = \sum_{\boldsymbol{q}}\sum_{\kappa=1}^{3}\boldsymbol{A}_{\boldsymbol{q}\kappa}\mathrm{e}^{\mathrm{i}(\omega_{q\kappa}t - \boldsymbol{R}\cdot\boldsymbol{q})}, \tag{14}$$

where $\boldsymbol{R}$ are the position vector of the atom in real space.

The corresponding velocity is

$$\boldsymbol{V}(\boldsymbol{R}) = \mathrm{i}\sum_{\boldsymbol{q}}\sum_{\kappa=1}^{3}\omega_{\boldsymbol{q}\kappa}\boldsymbol{A}_{\boldsymbol{q}\kappa}\mathrm{e}^{\mathrm{i}(\omega_{q\kappa}t - \boldsymbol{R}\cdot\boldsymbol{q})}. \tag{15}$$

The conjugate of the velocity becomes

$$\boldsymbol{V}^*(\boldsymbol{R}) = -\mathrm{i}\sum_{\boldsymbol{q}}\sum_{\kappa=1}^{3}\omega_{\boldsymbol{q}\kappa}\boldsymbol{A}^*_{\boldsymbol{q}\kappa}\mathrm{e}^{-\mathrm{i}(\omega_{q\kappa}t - \boldsymbol{R}\cdot\boldsymbol{q})}. \tag{16}$$

We have

$$\boldsymbol{V}\cdot\boldsymbol{V}^* = \sum_{\boldsymbol{q},\boldsymbol{q}'}\sum_{\kappa,\kappa'=1}^{3}\omega_{\boldsymbol{q}\kappa}\omega_{\boldsymbol{q}'\kappa'}\boldsymbol{A}_{\boldsymbol{q}\kappa}\bullet\boldsymbol{A}^*_{\boldsymbol{q}'\kappa'}\,\mathrm{e}^{\mathrm{i}(\omega_{q\kappa} - \omega_{q'\kappa'})t}\mathrm{e}^{\mathrm{i}\boldsymbol{R}\cdot(\boldsymbol{q}'-\boldsymbol{q})}. \tag{17}$$

The kinetic energy is

$$\frac{m}{2}\sum_{\boldsymbol{R}}\boldsymbol{V}\cdot\boldsymbol{V}^* = \frac{m}{2}\sum_{\boldsymbol{R}}\sum_{\boldsymbol{q},\boldsymbol{q}'}\sum_{\kappa,\kappa'=1}^{3}\omega_{\boldsymbol{q}\kappa}\omega_{\boldsymbol{q}'\kappa'}\boldsymbol{A}_{\boldsymbol{q}\kappa}\cdot\boldsymbol{A}^*_{\boldsymbol{q}'\kappa'}\,\mathrm{e}^{\mathrm{i}(\omega_{q\kappa} - \omega_{q'\kappa'})t}\mathrm{e}^{\mathrm{i}\boldsymbol{R}\cdot(\boldsymbol{q}'-\boldsymbol{q})}. \tag{18}$$

It is easy to verify [15]

$$\sum_{\boldsymbol{R}}e^{i\boldsymbol{R}\cdot\boldsymbol{S}} = \begin{cases}0, & \boldsymbol{S}\neq 0,\\ N, & \boldsymbol{S} = 0.\end{cases}$$

Hence the kinetic energy of the parallelepiped crystal equals

$$T_{\text{kinetic}} = N\frac{m}{2}\sum_{\boldsymbol{q}}\sum_{\kappa,\kappa'=1}^{3}\omega_{\boldsymbol{q}\kappa}\omega_{\boldsymbol{q}\kappa'}\boldsymbol{A}_{\boldsymbol{q}\kappa}\cdot\boldsymbol{A}^*_{\boldsymbol{q}'\kappa'}\mathrm{e}^{\mathrm{i}(\omega_{q\kappa} - \omega_{q\kappa'})t}. \tag{19}$$

Eq. (20) can be rewritten as:

$$T_{\text{kinetic}} = N\frac{m}{2}\sum_{\boldsymbol{q}}\boldsymbol{C}_{\boldsymbol{q}}(t)\cdot\boldsymbol{C}^{*}_{\boldsymbol{q}}(t),$$
$$\boldsymbol{C}_{\boldsymbol{q}}(t) = \sum_{\kappa=1}^{3}\omega_{\boldsymbol{q}\kappa}\boldsymbol{A}_{\boldsymbol{q}\kappa}\mathrm{e}^{\mathrm{i}\omega_{q\kappa}t}. \tag{20}$$

Let us consider the initial vector $\boldsymbol{C}_{\boldsymbol{q}}(0) = \sum_{\kappa=1}^{3}\omega_{\boldsymbol{q}\kappa}\boldsymbol{A}_{\boldsymbol{q}\kappa}$. One can put in throw statistic distribution. The vector $\boldsymbol{C}_{\boldsymbol{q}}(0)$ can be assimilated as velocity vector. The Maxwells distribution law can be used in simulations.

The Cauchy stress is given by Diao et al. [23],

$$\sigma_{\alpha\beta} = \frac{1}{V}\left[-\sum_{i} m_i \mathrm{V}_{i\alpha}\mathrm{V}_{i\beta} + \frac{1}{2}\sum_{i}\sum_{j\neq i} f_{ij\alpha}r_{ij\beta}\right], \tag{21}$$

where V is the volume of the crystal, m_i and V_i are the mass and velocity of atom i. $f_{ij\alpha}$ is the force between atom i and atom j. Subscriptions α, β denote the components in rectangular coordinate.

1.3 Effect of boundary condition

The solution (11) to dynamics equation (9) does not satisfy the real boundary condition for the parallelepiped crystal.

For monatomic crystal, the solution (11) can be rewritten as:

$$\boldsymbol{u}_j = \boldsymbol{A}\mathrm{e}^{\mathrm{i}(\omega t - \boldsymbol{R}_j\cdot\boldsymbol{q})},$$

where the R_j is the position vector of atom j.

Now we discuss a possible solution with the following form:

$$\boldsymbol{u}_j = [A\sin(\boldsymbol{R}_j\cdot\boldsymbol{q}_1) + B\cos(\boldsymbol{R}_j\cdot\boldsymbol{q}_1)]\mathrm{e}^{\mathrm{i}(\omega t - \boldsymbol{R}_j\cdot\boldsymbol{q}_2)}, \tag{22}$$

where

$$\boldsymbol{q}_1 = \frac{k_1}{N_1}\boldsymbol{b}_1,\quad \boldsymbol{q}_2 = \frac{k_2}{N_2}\boldsymbol{b}_2 + \frac{k_3}{N_3}\boldsymbol{b}_3. \tag{23}$$

Substituting eq. (22) into eq. (9) one obtains

$$\begin{aligned}&-m_k\omega^2[\boldsymbol{A}\sin(\boldsymbol{R}_k\cdot\boldsymbol{q}_1) + \boldsymbol{B}\cos(\boldsymbol{R}_k\cdot\boldsymbol{q}_1)]\\ &= \sum_{j\in\Omega_k}\boldsymbol{K}(r_{kj})\cdot\{[\boldsymbol{A}\sin(\boldsymbol{R}_j\cdot\boldsymbol{q}_1) + \boldsymbol{B}\cos(\boldsymbol{R}_j\cdot\boldsymbol{q}_1)]\mathrm{e}^{\mathrm{i}(\boldsymbol{R}_k-\boldsymbol{R}_j)\cdot\boldsymbol{q}_2}\\ &\quad -[\boldsymbol{A}\sin(\boldsymbol{R}_k\cdot\boldsymbol{q}_1) + \boldsymbol{B}\cos(\boldsymbol{R}_k\cdot\boldsymbol{q}_1)]\}.\end{aligned} \tag{24}$$

We note that

$$\begin{aligned}\sin(\boldsymbol{R}_j\cdot\boldsymbol{q}_1) &= \sin(\boldsymbol{R}_k\cdot\boldsymbol{q}_1)\cos(\boldsymbol{r}_{kj}\cdot\boldsymbol{q}_1)\\ &\quad + \cos(\boldsymbol{R}_k\cdot\boldsymbol{q}_1)\sin(\boldsymbol{r}_{kj}\cdot\boldsymbol{q}_1),\\ \cos(\boldsymbol{R}_j\cdot\boldsymbol{q}_1) &= \cos(\boldsymbol{R}_k\cdot\boldsymbol{q}_1)\cos(\boldsymbol{r}_{kj}\cdot\boldsymbol{q}_1)\\ &\quad - \sin(\boldsymbol{R}_k\cdot\boldsymbol{q}_1)\sin(\boldsymbol{r}_{kj}\cdot\boldsymbol{q}_1).\end{aligned}$$

Eq. (25) becomes

$$\begin{aligned}&-m_k\omega^2[\boldsymbol{A}\sin(\boldsymbol{R}_k\cdot\boldsymbol{q}_1) + \boldsymbol{B}\cos(\boldsymbol{R}_k\cdot\boldsymbol{q}_1)]\\ &= \sum_{j\in\Omega_k}\boldsymbol{K}(r_{kj})\cdot\{[\boldsymbol{A}\sin(\boldsymbol{R}_k\cdot\boldsymbol{q}_1) + \boldsymbol{B}\cos(\boldsymbol{R}_k\cdot\boldsymbol{q}_1)]\\ &\quad\times\cos(\boldsymbol{r}_{kj}\cdot\boldsymbol{q}_1)\mathrm{e}^{\mathrm{i}(\boldsymbol{R}_k-\boldsymbol{R}_j)\cdot\boldsymbol{q}_2}\\ &\quad -[\boldsymbol{A}\sin(\boldsymbol{R}_k\cdot\boldsymbol{q}_1) + \boldsymbol{B}\cos(\boldsymbol{R}_k\cdot\boldsymbol{q}_1)]\\ &\quad +[\boldsymbol{A}\cos(\boldsymbol{R}_k\cdot\boldsymbol{q}_1) - \boldsymbol{B}\sin(\boldsymbol{R}_k\cdot\boldsymbol{q}_1)]\sin(\boldsymbol{r}_{kj}\cdot\boldsymbol{q}_1)\mathrm{e}^{\mathrm{i}(\boldsymbol{R}_k-\boldsymbol{R}_j)\cdot\boldsymbol{q}_2}.\end{aligned} \tag{25}$$

In order to explain the contents more clearly, let us consider a crystal with face-centered cubic lattice and take into account only the interaction from the nearest neighbor atoms as shown in Figure 2. According to the Cauchy-Born law, all atoms within the face-centered cubic crystal are in the static equilibrim positions after homogeous deformation. We have

$$r_{01} = r_{03},\ r_{02} = r_{04},\ r_{05} = r_{07},\ r_{06} = r_{08},\ r_{09} = r_{011},\ r_{010} = r_{012}.$$

Now eq. (25) is reduced to

$$\begin{aligned}&m\omega^2[\boldsymbol{A}\sin(\boldsymbol{R}_k\cdot\boldsymbol{q}_1) + \boldsymbol{B}\cos(\boldsymbol{R}_k\cdot\boldsymbol{q}_1)]\\ &= \sum_{j\in\Omega_0}\boldsymbol{K}(r_{kj})\cdot\{[\boldsymbol{A}\sin(\boldsymbol{R}_k\cdot\boldsymbol{q}_1) + \boldsymbol{B}\cos(\boldsymbol{R}_k\cdot\boldsymbol{q}_1)]\\ &\quad\times 2[1-\cos(\boldsymbol{r}_{kj}\cdot\boldsymbol{q}_1)\cos(\boldsymbol{r}_{kj}\cdot\boldsymbol{q}_2)]\\ &\quad +[\boldsymbol{A}\cos(\boldsymbol{R}_k\cdot\boldsymbol{q}_1) - \boldsymbol{B}\sin(\boldsymbol{R}_k\cdot\boldsymbol{q}_1)]\\ &\quad\times 2\mathrm{i}\sin(\boldsymbol{r}_{kj}\cdot\boldsymbol{q}_1)\sin(\boldsymbol{r}_{kj}\cdot\boldsymbol{q}_2)\},\\ &\quad \Omega_0 = 1,\ 2,\ 5,\ 6,\ 9,\ 10.\end{aligned} \tag{26}$$

It is easy to verify that the term $\sin(\boldsymbol{r}_{kj}\cdot\boldsymbol{q}_1)\sin(\boldsymbol{r}_{kj}\cdot\boldsymbol{q}_2)$ in the above equation equals zero for each $j\in\Omega_0$. Then the above equation becomes

$$\begin{aligned}&m\omega^2[\boldsymbol{A}\sin(\boldsymbol{R}_k\cdot\boldsymbol{q}_1) + \boldsymbol{B}\cos(\boldsymbol{R}_k\cdot\boldsymbol{q}_1)]\\ &= \sum_{j\in\Omega_0}\boldsymbol{K}(r_{kj})\cdot\{[\boldsymbol{A}\sin(\boldsymbol{R}_k\cdot\boldsymbol{q}_1) + \boldsymbol{B}\cos(\boldsymbol{R}_k\cdot\boldsymbol{q}_1)]\\ &\quad\times 2[1-\cos(\boldsymbol{r}_{kj}\cdot\boldsymbol{q}_1)\cos(\boldsymbol{r}_{kj}\cdot\boldsymbol{q}_2)]\}\end{aligned}$$

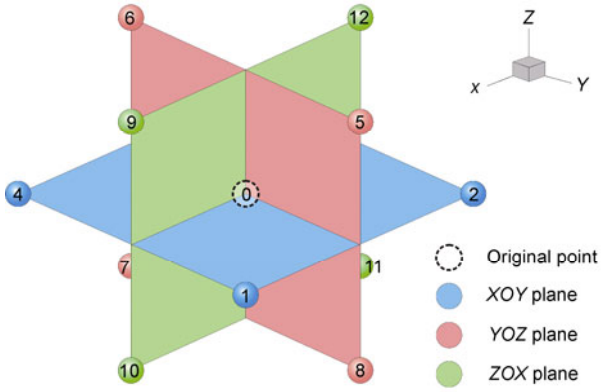

Figure 2 Three-dimensional crystal of face cetraled cubic Cu.

$$= \sum_{j\in\Omega_0} \boldsymbol{K}(r_{kj})\cdot\{[\boldsymbol{A}\sin(\boldsymbol{R}_k\cdot\boldsymbol{q}_1)+\boldsymbol{B}\cos(\boldsymbol{R}_k\cdot\boldsymbol{q}_1)] \times 2[1-\cos(\boldsymbol{r}_{kj}\cdot\boldsymbol{q})]\}. \quad (27)$$

Eq. (28) can be rewritten as follows:

$$m\omega^2\boldsymbol{C} = \sum_{j\in\Omega_0} \boldsymbol{K}(r_{kj})\cdot\boldsymbol{C}\,2[1-\cos(\boldsymbol{r}_{kj}\cdot\boldsymbol{q})], \quad (28)$$

where

$$\boldsymbol{C} = \boldsymbol{A}\sin(\boldsymbol{R}_k\cdot\boldsymbol{q}_1)+\boldsymbol{B}\cos(\boldsymbol{R}_k\cdot\boldsymbol{q}_1). \quad (29)$$

Eq. (28) is identical to eigen equation (13). This means that the solution (23) is really the solution to dynamic equation (9).

The position vector $\boldsymbol{R}$ of atoms can be expressed as:

$$\boldsymbol{R} = l_1\boldsymbol{a}_1 + l_2\boldsymbol{a}_2 + l_3\boldsymbol{a}_3, \quad (30)$$

where l_1, l_2, l_3 are the integers which obey the following condition:

$$0 \leqslant l_1 \leqslant N_1,\ \ 0 \leqslant l_2 \leqslant N_2,\ \ 0 \leqslant l_3 \leqslant N_3.$$

The solution (22) can be rewritten as:

$$\begin{aligned}\boldsymbol{u}(\boldsymbol{R}) &= [A\sin(\boldsymbol{R}\cdot\boldsymbol{q}_1)+B\cos(\boldsymbol{R}\cdot\boldsymbol{q}_1)]\mathrm{e}^{\mathrm{i}(\omega t-\boldsymbol{R}\cdot\boldsymbol{q}_2)}\\ &= [A\sin(2\pi\xi_1 l_1)+B\cos(2\pi\xi_1 l_1)]\mathrm{e}^{\mathrm{i}(\omega t-\boldsymbol{R}\cdot\boldsymbol{q}_2)}, \quad (31)\\ \xi_1 &= \frac{k_1}{N_1}.\end{aligned}$$

The rectangular parallelepiped occupies the space

$$0 \leqslant x \leqslant N_1 a_1,\ \ 0 \leqslant y \leqslant N_2 a_2,\ \ 0 \leqslant z \leqslant N_3 a_3.$$

The solution for different boundary conditions at $x = 0$ ($l_1 = 0$) and $x = N_1 a_1$ ($l_1 = N_1$) can be listed as follows:

Periodic boundary condition:

$$\begin{aligned}\boldsymbol{u}(\boldsymbol{R}) &= [A\sin(\boldsymbol{R}\cdot\boldsymbol{q}_1)+B\cos(\boldsymbol{R}\cdot\boldsymbol{q}_1)]\mathrm{e}^{\mathrm{i}(\omega t-\boldsymbol{R}\cdot\boldsymbol{q}_2)}\\ &= [A\sin(2\pi\xi_1 l_1)+B\cos(2\pi\xi_1 l_1)]\mathrm{e}^{\mathrm{i}(\omega t-\boldsymbol{R}\cdot\boldsymbol{q}_2)},\\ \xi_1 &= \frac{k_1}{N_1},\quad k_1 = 1,\ 2,\ 3,\ ...,\ N_1. \quad (32)\end{aligned}$$

Fixed boundary condition:

$$\begin{aligned}\boldsymbol{u}(\boldsymbol{R}) &= A\sin(\boldsymbol{R}\cdot\boldsymbol{q}_1)\mathrm{e}^{\mathrm{i}(\omega t-\boldsymbol{R}\cdot\boldsymbol{q}_2)}\\ &= A\sin(2\pi\xi_1 l_1)\mathrm{e}^{\mathrm{i}(\omega t-\boldsymbol{R}\cdot\boldsymbol{q}_2)},\\ \xi_1 &= \frac{k_1}{N_1},\quad k_1 = 1,\ 2,\ 3,\ ...,\ \frac{N_1}{2}. \quad (33)\end{aligned}$$

Free boundary condition:

$$\begin{aligned}\boldsymbol{u}(\boldsymbol{R}) &= B\cos(\boldsymbol{R}\cdot\boldsymbol{q}_1-\pi\mathrm{q}_1)]\mathrm{e}^{\mathrm{i}(\omega t-\boldsymbol{R}\cdot\boldsymbol{q}_2)}\\ &= B\cos\left[2\pi\xi_1\left(l_1-\frac{1}{2}\right)\right]\mathrm{e}^{\mathrm{i}(\omega t-\boldsymbol{R}\cdot\boldsymbol{q}_2)}\\ \xi_1 &= \frac{k_1}{N_1},\quad k_1 = 1,\ 2,\ 3,\ ...,\ \frac{N_1}{2}. \quad (34)\end{aligned}$$

From the above equations, one can clearly see that the different boundary conditions at $x = 0$ ($l_1 = 0$) and $x = N_1 a_1$ ($l_1 = N_1$) have no effects on the eigen-equation (13) and the frequency spectrum of the parallelepiped crystal. But the distribution interval of the wave numbers is different for different boundary conditions

Similarly one can prove that the different boundary conditions at $y = 0$ ($l_2 = 0$) and $y = N_2 a_2$ ($l_2 = N_2$) and at z=0 and $z = N_3 a_3$ ($l_3 = N_3$) have no effects on the eigen-equation (13) and the frequency spectrum of the parallelepiped crystal.

2 Thermodynamic properties of crystal

2.1 Specific heat

The specific heat C_V is defined as the heat energy required per unit volume of solid per degree of temperature change at constant volume. We have the following formula [21,22]:

$$C_\mathrm{V} = \left(\frac{\partial E_\mathrm{tot}}{\partial T}\right)_V, \quad (35)$$

where the E_tot is the total thermal energy of the system of N atoms, which is the sum of contribution from all harmonic oscillators.

$$E = \sum_{j=1}^{3N}\overline{E}_j,\ \ \overline{E}_j = \frac{1}{2}\hbar\omega_j + \frac{\hbar\omega_j}{\mathrm{e}^{\hbar\omega_j/k_BT}-1}. \quad (36)$$

We have

$$C_\mathrm{V} = \sum_{j=1}^{3N}\frac{\mathrm{d}\overline{E}_j(T)}{\mathrm{d}T} = \sum_{j=1}^{3N}k_\mathrm{B}\frac{\left(\frac{\hbar\omega_j}{k_\mathrm{B}T}\right)^2\mathrm{e}^{\hbar\omega_j/k_\mathrm{B}T}}{\left(\mathrm{e}^{\hbar\omega_j/k_\mathrm{B}T}-1\right)^2}, \quad (37)$$

where $\hbar$ is the reduced Planck's constant, k_B is the Boltzmann constant, N is the atom number of underlying crystal, and the vibration frequency ω_j of the jth normal mode of the crystal lattice depends only on the lattice deformation for the harmonic approximation.

The modified L-J inter-atomic potential for single crystal Cu takes the form:

$$\begin{aligned}\phi &= 4\varepsilon\left\{\left[\left(\frac{\sigma}{r}\right)^{12}-\left(\frac{\sigma}{r}\right)^{6}\right]+\phi_1(r)\right\},\\ \phi_1(r) &= \beta_1\left[\left(\frac{\sigma}{r}\right)^{12}-\gamma_0\left(\frac{\sigma}{r}\right)^{6}\right].\end{aligned} \quad (38a)$$

The parameter γ_0 is determined from the requirement $\phi_1''(r)_{r=R}=0$, and $R=\frac{\sqrt{2}}{2}a_0$, a_0 is the crystal constant of Cu. Therefore the parameter ε can be determined from the elastic volume modulus K_0, $K_0=137$ GPa [24]. The parameter β_1 is used to adjust the first-order derivative of the potential function $\phi(r)$. We have

$$\begin{aligned}&\sigma=2.255\ \text{Å},\quad \varepsilon=0.2554\ \text{eV},\\ &\gamma_0=\frac{26}{7}\left(\frac{\sigma}{R}\right)^6,\ \beta_1=10.13\left(\frac{R}{\sigma}\right)^{12}.\end{aligned}\tag{38b}$$

The vibration frequencies are calculated based on eq. (13) and only the inter-atomic potential from the nearest neighbor atoms is taken into account. Figure 3 shows the comparison between the calculation results and experimental data. The rhombus with blue color is the experimental data given by Billings and Gray [25]; the black square is the present calculation result, in which the average frequency is taken to be the Einstein's frequency ω_0; the small circle with red color is the present calculation result in which the average thermo energy is taken to be the thermo energy of Einstein's single frequency model, and the triangle with green color is the present calculation result given by eq. (37).

One can clearly see that the three calculation results are consistent with each other and agree well with the experimental data. When the temperature is higher than the room temperature, the present calculation results deviate gradually from the experimental data. This means that the an-harmonic effect needs to be considered at a high temperature.

2.2 Coefficient of thermal expansion

According to the Grüneisen's law [21,22], the coefficient of thermal expansion α can be expressed as:

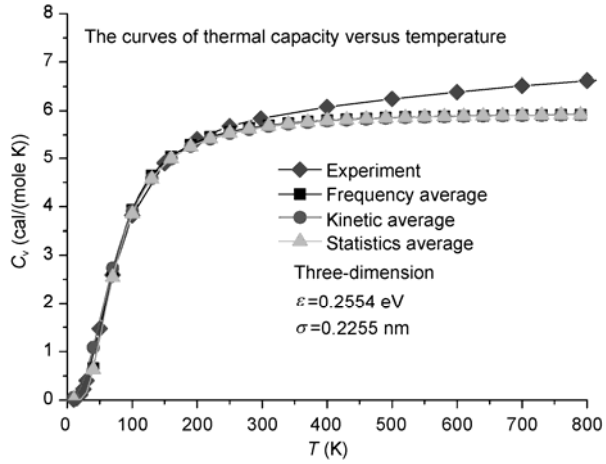

Figure 3 Temperature dependence of specific heat for single crystal Cu.

$$\alpha=\frac{1}{3}\alpha_{\mathrm{V}}=\frac{\gamma}{3K_0}\frac{C_{\mathrm{V}}}{V},\tag{39}$$

where the γ is the Grüneisen's constant, K_0 is the elastic volume modulus of the crystal and C_{V} is the specific heat at constant volume.

Figure 4 shows the comparison of present calculation results with the experimental data [25] for crystal Cu. The Grüneisen's constant γ is taken to be 2.0.

3 Quantum theory of thermal stress of crystal

3.1 Helmholtz free energy

The Helmholtz free energy is given by Ziman [22]

$$\begin{aligned}&F=U+k_{\mathrm{B}}T\sum_{i=1}^{3N}\ln\left[2\sinh\left(\frac{1}{2}\beta\hbar\omega_i\right)\right],\\ &\beta=1/k_{\mathrm{B}}T.\end{aligned}\tag{40}$$

The second Piola-Kirchhoff stress is determined by

$$S_{\alpha\beta}=\frac{1}{V_0}\frac{\partial F}{\partial\varepsilon_{\alpha\beta}}=\left\{\frac{\partial U}{\partial\varepsilon_{\alpha\beta}}+\sum_i\frac{\overline{E_i}}{\omega_i}\cdot\frac{\partial\omega_i}{\partial\varepsilon_{\alpha\beta}}\right\}\Big/V_0,\tag{41}$$

where $\varepsilon_{\alpha\beta}$ is the Green strain, U is the potential energy, ω_i is the frequency, and $\overline{E}_i$ is the thermo energy of the ith normal mode of the lattice vibration. The Cauchy stress takes the form

$$\boldsymbol{\sigma}=\boldsymbol{F}\left\{\frac{\partial U}{\partial\boldsymbol{\varepsilon}}+\sum_i\frac{\overline{E_i}}{\omega_i}\cdot\frac{\partial\omega_i}{\partial\boldsymbol{\varepsilon}}\right\}\boldsymbol{F}^{\mathrm{T}}/V,\tag{42}$$

where $\boldsymbol{F}$ is the deformation gradient.

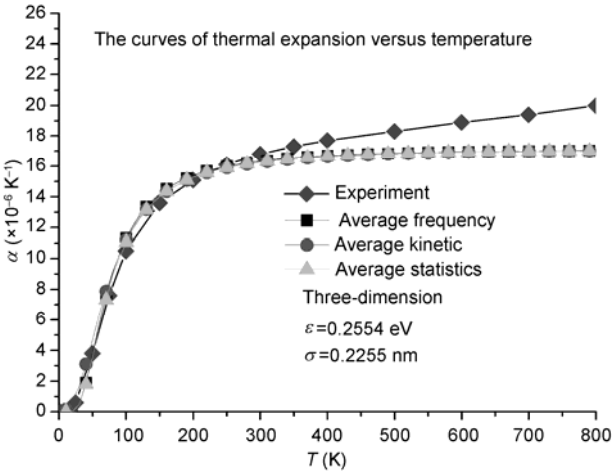

Figure 4 Thermal expansion versus temperature for crystal Cu. Three calculation results (due to three calculation results of C_{V}) based on eq. (40) are included and compared with experimental data [25]. The Grüneisen's constant γ is taken to be 2.0.

If the plastic deformation is taken into account, the Cauchy stress can be expressed as:

$$\boldsymbol{\sigma} = \boldsymbol{F}^{\mathrm{e}} \left\{ \frac{\partial U}{\partial \boldsymbol{\varepsilon}^{\mathrm{e}}} + \sum_i \frac{\overline{E_i}}{\omega_i} \cdot \frac{\partial \omega_i}{\partial \boldsymbol{\varepsilon}^{\mathrm{e}}} \right\} (\boldsymbol{F}^{\mathrm{e}})^{\mathrm{T}} / V, \tag{43}$$

where $\boldsymbol{F}^{\mathrm{e}}$ is the elastic deformation gradient from the intermediate configuration to the current configuration, and $\boldsymbol{\varepsilon}^{\mathrm{e}}$ is the elastic strain. Since the plastic slip has no effect on the crystal lattice and the elastic distortion of the crystal lattice is quite small, eq. (43) is reduced to

$$\boldsymbol{\sigma} = \left\{ \frac{\partial U}{\partial \boldsymbol{\varepsilon}^{\mathrm{e}}} + \sum_i \frac{\overline{E_i}}{\omega_i} \cdot \frac{\partial \omega_i}{\partial \boldsymbol{\varepsilon}^{\mathrm{e}}} \right\} / V. \tag{44}$$

For uniaxial tension, eq. (45) becomes

$$\sigma = \left\{ \frac{\partial U}{\partial \varepsilon^{\mathrm{e}}} + \sum_i \frac{\overline{E_i}}{\omega_i} \cdot \frac{\partial \omega_i}{\partial \varepsilon^{\mathrm{e}}} \right\} / V. \tag{45}$$

3.2 The modified inter-atomic potential

As pointed by Jiang and Huang [11], the coefficient of thermal expansion is proportional to the third-order derivative of the potential energy. Hence the Cauchy stress also depends on the third-order derivative of the potential energy. Therefore the inter-atomic potential needs to be modified to include the effect of the third-order derivative of the potential energy. The detailed procedure is given in Appendix.

3.3 Thermal stress of copper

The experiment study for the influence of temperature on the stress-strain relationship of copper and copper alloy was carried out by McAdam [26]. A typical experimental result of flow stress curves with Copper was shown in Figure 3 of his paper. Five experimental curves of the flow stresses corresponding to different temperatures were obtained. Each curve represents the incipient-flow stress at the indicated temperature, which was derived from the standard stress-strain curve at room temperature under the same true strain when the temperature was raised (or dropped down) to the indicated temperature.

The standard stress-strain curve at room temperature for Copper given by McAdam [26] can be described by the following formula:

$$\varepsilon_{\mathrm{true}} = B\left(\frac{\sigma}{\sigma_{\mathrm{ys}}}\right) = \begin{cases} \dfrac{\sigma}{E}, & \varepsilon_{\mathrm{true}} \leqslant \varepsilon_{\mathrm{ys}}, \\ \sigma = \sigma_{\mathrm{ys}}, & \varepsilon_{\mathrm{ys}} \leqslant \varepsilon_{\mathrm{true}} \leqslant \varepsilon_{\mathrm{ys}}^{*}, \\ \dfrac{\sigma}{E_{\mathrm{p}}} + \alpha \left(\dfrac{\sigma}{\sigma_{\mathrm{ys}}}\right)^{m} & \varepsilon_{\mathrm{ys}}^{*} \leqslant \varepsilon_{\mathrm{true}}, \end{cases} \tag{46}$$

where E is the elastic modulus, σ_{ys} is the yield stress, $\varepsilon_{\mathrm{ys}} = \sigma_{\mathrm{ys}} / E$, $\varepsilon_{\mathrm{ys}}^{*} = \sigma_{\mathrm{ys}} / E_{\mathrm{p}} + \alpha$, the parameters E_{p}, α, m are determined by the fitting procedure from the standard stress-strain curve at room temperature for Copper. Only the second part of the standard stress-strain curve for $\varepsilon_{\mathrm{true}} > \varepsilon_{\mathrm{ys}}^{*}$ is used in the fitting procedure. According to the experimental data [26], the elastic modulus and the yield stress are chosen to be $E = 102$ GPa, $\sigma_{ys} = 69.79$ MPa. The fitting parameters are:

$$E_{\mathrm{p}} = 2.923 \text{ GPa}, \ \alpha = 2.653 \times 10^{-6}, \ m = 7.5.$$

From eq. (46) one gets

$$\sigma = \sigma_{\mathrm{ys}} A(\varepsilon_{\mathrm{true}}), \tag{47}$$

where the function $A(\varepsilon_{\mathrm{true}})$ is the inverse function of the function $B(\sigma / \sigma_{\mathrm{ys}})$.

Comparing eqs. (45) and (47), one obtains

$$\sigma = \sigma_{\mathrm{ys}} A(\varepsilon_{\mathrm{true}}) = \left\{ \left[\frac{\partial U}{\partial \varepsilon^{e}} + \sum_i \frac{\overline{E_i}}{\omega_i} \cdot \frac{\partial \omega_i}{\partial \varepsilon^{e}} \right] / V \right\}_{t=23^{\circ}\mathrm{C}}. \tag{48}$$

Based on the above equation, eq. (46) can be rewritten as follows:

$$\sigma = \sigma_{\mathrm{ys}} A(\varepsilon_{\mathrm{true}}) + \left\{ \frac{\partial U}{\partial \varepsilon^{e}} + \sum_i \frac{\overline{E_i}}{\omega_i} \cdot \frac{\partial \omega_i}{\partial \varepsilon^{\mathrm{e}}} \right\} / V - \left\{ \left[\frac{\partial U}{\partial \varepsilon^{e}} + \sum_i \frac{\overline{E_i}}{\omega_i} \cdot \frac{\partial \omega_i}{\partial \varepsilon^{e}} \right] / V \right\}_{t=23^{\circ}\mathrm{C}}. \tag{49}$$

Since the potential U is independent of temperature, eq. (49) becomes

$$\sigma = \sigma_{ys} A(\varepsilon_{\mathrm{true}}) + \left[\sum_i \frac{\overline{E_i}}{\omega_i} \cdot \frac{\partial \omega_i}{\partial \varepsilon^{e}} \right] / V - \left\{ \left[\sum_i \frac{\overline{E_i}}{\omega_i} \cdot \frac{\partial \omega_i}{\partial \varepsilon^{e}} \right] / V \right\}_{T=23^{\circ}\mathrm{C}.}. \tag{50}$$

The calculation results of eq. (50) are shown in Figures 5–7.

The flow stress at room temperature is shown in Figure 5, where the black square is the experimental data [26], and the red circle is the fitting curve of eq. (46). The fitting curve matches the experimental data very well.

The flow stresses at temperatures $T = 100^{\circ}\mathrm{C}$ and $T = -128^{\circ}\mathrm{C}$ are shown in Figures 6(a) and (b), respectively. The black square is the experimental data [26], and the red circle is the present calculation result of eq. (50). The calculation results agree well with the experimental data.

Figures 7(a) and (b) show the flow stresses at temperatures $T = 165^{\circ}\mathrm{C}$ and $T = -188^{\circ}\mathrm{C}$, respectively.

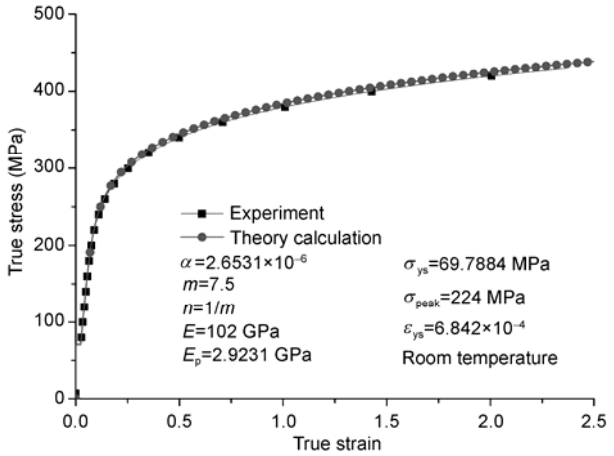

Figure 5 The comparison between the fitting curve and the experimental data [26] of flow stress for copper at room temperature.

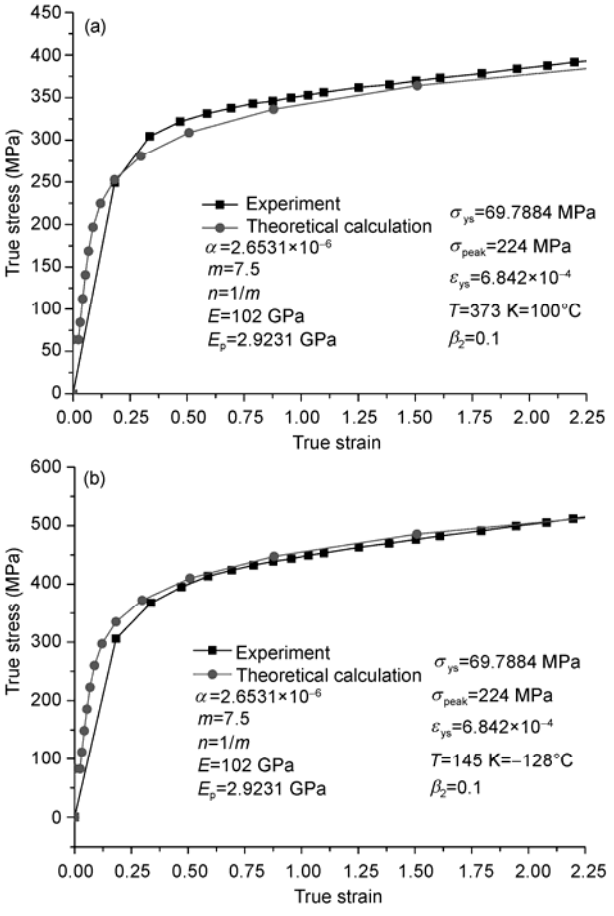

Figure 6 (a) Flow stress versus true strain for copper at temperature T=100°C. The black square is the experimental data [26], and the red circle is the present calculation result of eq. (50). (b) The comparison of the flow stress for copper between the calculation result of eq. (55) and the experimental data [26] at temperature T=−128°C.

From these figures one can see that the present calculation results based on eq. (50) are in good agreement with the experimental data [26].

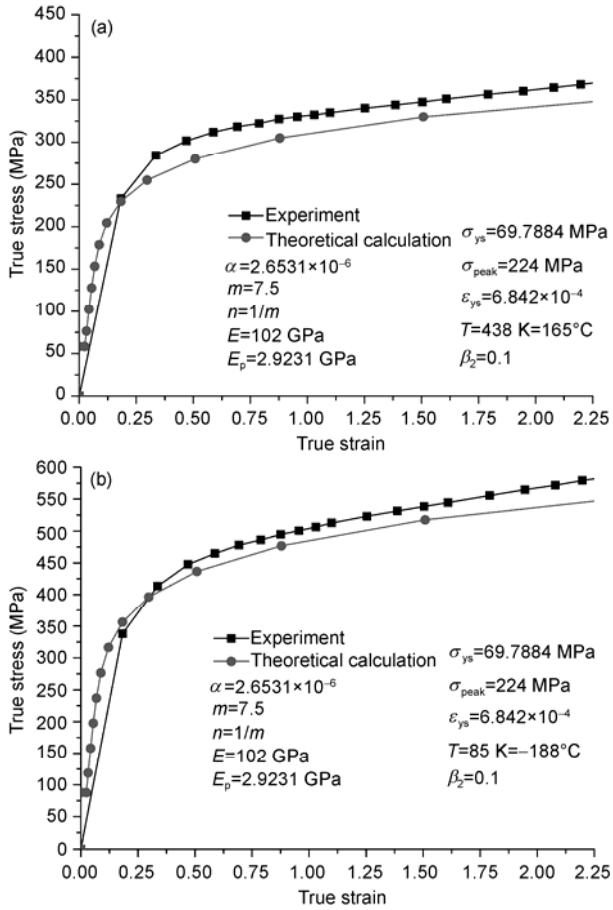

Figure 7 (a) Flow stress versus true strain for copper at temperature T=165°C. (b) Variation of the flow stress for copper at temperature T=−188°C.

The deviation from the experimental data is less than 8% for $T = 165$°C and 7% for $T = -188$°C.

4 Conclusion

In this paper, we propose an effective method to study the thermodynamic properties and constitutive relations of crystals at finite temperature based on the theory of lattice dynamics [15] and interatomic potential of EAM model [19]. The exact dynamics equation for each individual atom is established directly around the equilibrium state of the system of N atoms. Using harmonic approximation and periodical boundary condition, the $3N\times3N$ force constant matrix of the parallelepiped crystal is reduced to a $3n\times3n$ force constant matrix for the unit cell.

By the present method, the thermodynamic properties for Cu are calculated, and found in very good agreement with the experimental data.

Finally the present theory is extended to include the effect of plastic deformation. The stress-strain relationships of copper with large plastic deformation at different tempera-

tures are calculated. The predictions of the preset theory agree well with experimental data.

Appendix

The modified L-J potential can be expressed as:

$$\phi = 4\varepsilon\left\{\left[\left(\frac{\sigma}{r}\right)^{12} - \left(\frac{\sigma}{r}\right)^{6}\right] + \phi_1(r) + \phi_2(r)\right\}. \tag{a1}$$

The potential energy $\phi_1(r)$ has been given in eq. (39), which takes the form:

$$\begin{aligned} &\phi_1(r) = \beta_1\left[\left(\frac{\sigma}{r}\right)^{12} - \gamma_0\left(\frac{\sigma}{r}\right)^{6}\right], \\ &\gamma_0 = \frac{26}{7}\left(\frac{\sigma}{R}\right)^{6}, \\ &\beta_1 = 10.128\left(\frac{R}{\sigma}\right)^{12}. \end{aligned} \tag{a2}$$

The potential energy $\phi_2(r)$ is assumed to be equal to

$$\phi_2(r) = \beta_2\left[\left(\frac{R}{r}\right)^{12} + \gamma_1\left(\frac{R}{r}\right)^{9} + \gamma_2\left(\frac{R}{r}\right)^{6}\right], \tag{a3}$$

where R is the first nearest, $R = \sqrt{2}a_0/2$.

The parameters γ_1 and γ_2 are determined from the following equations:

$$\phi_2'(r)_{r=R} = \phi_2''(r)_{r=R} = 0. \tag{a4}$$

The parameters $\gamma_1 = -8/3$ and $\gamma_2 = 2$. And β_2 is used to adjust the third-order derivative of the potential function $\phi(r)$. After adjustment, parameter β_2 is taken to be equal to be 0.1.

The research was supported by the National Natural Science Foundation of China (Grant Nos. 10872197, 11021262 and 11172303).

1 To A C, Liu W K, Kopacz A. A finite temperature continuum theory based on interatomic potential in crystalline solids. Comput Mech, 2008, 42: 531–541
2 Tadmor E B, Ortiz M, Phillips R. Quasicontinuum analysis of defects in solids. Philos Mag A, 1996, 73: 1529–1563
3 Tadmor E B, Phillips R, Ortiz M. Mixed atomistic and continuum models of deformation in solids. Langmuir, 1996, 12: 4529–4534
4 Shenoy V B, Miller R, Tadmor E B, et al. Quasicontinuum models of interfacial structure and deformation. Phys Rev Lett, 1998, 80: 742–745
5 Miller R, Ortiz M, Phillips R, et al. Quasicontinuum models of fracture and plasticity. Eng Fract Mech, 1998, 61: 427–444
6 Miller R, Tadmor E B, Phillips R, et al. Quasicontinuum simulation of fracture at the atomic scale. Model Simul Mater Sci, 1998, 6: 607–638
7 Shilkrot L E, Curtin W A, Miller R E. A coupled atomistic/ continuum model of defects in solids. J Mech Phys Solids, 2002, 50: 2085–2106
8 Shilkrot L E, Curtin W A, Miller R E. A coupled atomistic/ continuum model of defects in solids. J Mech Phys Solids, 2002, 50: 2085–2106
9 Gao H J, Klein P. Numerical simulation of crack growth in an isotropic solid with randomized internal cohesive bonds. J Mech Phys Solids, 46:187–218
10 Klein P, Gao H. Crack nucleation and growth as strain localization in a virtual-bond continuum. Eng Fract Mech, 1998, 61: 21–48
11 Jiang H, Huang Y, Hwang K C. A finite-temperature continuum theory based on interatomic potentials. J Eng Mater, 127: 408–416
12 Miller R E, Tadmor E. The quasicontinuum method: Overview, applications and current directions. J Comput-Aided Mater Design, 9: 203–239
13 Shenoy V, Phillips R. Finite temperature quasicontinuum methods. Mater Res Soc, 1999, 538: 465–471
14 Dupuy L M, Tadmor E B, Miller R E, et al. Finite-temperature quasicontinuum: Molecular dynamics without all the atoms. Phys Rev Lett, 2005, 95: 060202
15 Born M, Huang K. Dynamical Theory of Crystal Lattices. Oxford: Oxford University Press,1998
16 Ashcroft N W, Mermin N. Solid State Physics. Holt-Saunders: Tokyo, 1981
17 Tang Z, Zhao H, Li G, et al. Finite-temperature quasicontinuum method for multiscaleanalysis of silicon nanostructures. Phys Rev B, 2006, 74: 64110
18 Zhao H, Tang Z, Li G, et al. Quasiharmonic models for the calculation of thermodynamic properties of crystalline silicon under strain. J Appl Phys, 2006, 99: 064314
19 Daw M S, Baskes M I. Embedded-atom method—derivation and application to impurities, surfaces, and other defects in metals. Phys Rev B, 1984, 29: 6443–6453
20 Tang Q H, Wang T C. Lattice wave theory of molecular dynamics (in Chinese). Sci Sin-Phys Mech Astron, 2011, 41: 214–220
21 Huang, K, Han Y. Physics of Solid State (in Chinese). Beijing: Peking University Press, 1982
22 Ziman J M. Principles of the Theory of Solids. Cambridge: Cambridge Univ Press, 1979
23 Diao J K, Gall K, Dunn M L, et al. Atomistic simulations of the yielding of gold nanowires. Acta Mater, 2006, 54: 643–653
24 Kittel C. Introduvtion to Solid State Physics. 5th ed. New York: John Wiley & Sons, Inc., 1976; Billings B H, Gray D E. American Institute of Physics Handbook. 3rd ed. New York: McGraw-Hill, 1972
25 Brenner D W. Empirical potential for hydrocarbons for use in simulating the chemical vapor deposition of diamond films. Phys Rev B, 1990, 42: 9558
26 McAdam D J. Influence of temperature on the stress-strain-energy relationship for Copper and Nickel-Copper alloy. Metals Trans, 185: 727–740